Noninvasive quantification of postocclusive reactive hyperemia in mouse thigh muscle by near-infrared diffuse correlation spectroscopy

Ran Cheng,[1,†] Xiaoyan Zhang,[1,†] Alan Daugherty,[2] Hainsworth Shin,[1] and Guoqiang Yu[1,*]

[1]Department of Biomedical Engineering, University of Kentucky, 600 Rose Street, Lexington, Kentucky 40506, USA

[2]Saha Cardiovascular Research Center, University of Kentucky, 741 South Limestone Avenue, Lexington, Kentucky 40536, USA

*Corresponding author: guoqiang.yu@uky.edu

Received 19 June 2013; revised 22 August 2013; accepted 27 September 2013; posted 1 October 2013 (Doc. ID 192578); published 16 October 2013

Many vasculature-related diseases affecting skeletal muscle function have been studied in mouse models. Noninvasive quantification of muscle blood flow responses during postocclusive reactive hyperemia (PORH) is often used to evaluate vascular function in human skeletal muscles. However, blood flow measurements during PORH in small skeletal muscles of mice are rare due to the lack of appropriate technologies coupled with the challenge of measurement setup resulting from the lack of large enough test sites. In this study, we explored adapting diffuse correlation spectroscopy (DCS) for noninvasive measurement of the relative changes of blood flow (rBF) in mouse thigh muscles during PORH. A small fiber-optic probe was designed and glued on the mouse thigh to reduce the motion artifact induced by the occlusion procedure. Arterial occlusion was created by tying a polyvinyl chloride (PVC) tube around the mouse thigh while the muscle rBF was continuously monitored by DCS to ensure the success of the occlusion. After 5 min, the occlusion was rapidly released by severing the PVC tube using a cautery pen. Typical rBF responses during PORH were observed in all mice ($n = 7$), which are consistent with those observed by arterial-spin-labeled magnetic resonance imaging (ASL-MRI) as reported in the literature. On average, rBF values from DCS during occlusion were lower than 10% ($3.1 \pm 2.2\%$) of the baseline values (assigning 100%), indicating the success of arterial occlusion in all mice. Peak values of rBF during PORH measured by the DCS ($357.6 \pm 36.3\%$) and ASL-MRI ($387.5 \pm 150.0\%$) were also similar whereas the values of time-to-peak (the time duration from the end of occlusion to the peak rBF) were quite different (112.6 ± 35.0 s versus 48.0 ± 27.0 s). Simultaneous measurements by these two techniques are needed to identify the factors that may cause such discrepancy. This study highlights the utility of DCS technology to quantitatively evaluate tissue blood flow responses during PORH in mouse skeletal muscles. DCS holds promise as valuable tool to assess blood flow regulation in mouse models with a variety of vascular diseases (e.g., hypercholesterolemia, diabetes, peripheral artery disease).

OCIS codes: (170.0170) Medical optics and biotechnology; (170.3890) Medical optics instrumentation; (170.5380) Physiology; (170.6480) Spectroscopy, speckle.

http://dx.doi.org/10.1364/AO.52.007324

1. Introduction

Mice have been extensively used as an experimental animal model for studying human pathobiology because of their fully defined genome sequence, fast reproduction rate, low cost, and ease of handling. Many vasculature-related diseases affecting skeletal muscle functions, such as diabetes and peripheral arterial disease (PAD), have been studied in mouse models [1,2]. For example, Guo *et al.* evaluated diabetes-induced muscle dysfunction via *in vitro*

1559-128X/13/307324-07$15.00/0

assessment of the isometric contractions and the levels of cyclooxygenase-2 mRNA and protein in smooth muscles removed from mice [1]. Rufaihah *et al.* used *in vitro* immunofluorescence staining of ischemic muscle tissues to study the effect of stem cell therapy in a mouse model of PAD [2]. These methods, while effective, are invasive and end-point measures that capture only a "snapshot" of the muscle condition. Moreover, although these studies [1,2] revealed valuable mechanistic information, their impact on the dynamics of muscle blood flow regulation is lost.

Noninvasive quantification of muscle blood flow responses during postocclusive reactive hyperemia (PORH) is often used to evaluate vascular function in human skeletal muscles [3,4]. PORH refers to the hyperperfusion (usually higher than its baseline value) after the release of arterial occlusion. The hyperemic response during PORH involves a variety of vascular control factors including metabolic and endothelial vasodilation, myogenic response, and sensory nerve control [5,6], and thus can be used for vascular function assessment. For example, a peak flow $\leq$75% of the baseline and time for the hyperemia response to fall to 50% of the peak $\geq$40 s have been suggested to be two criteria in diagnosing PAD [7]. It is highly desirable to translate this noninvasive method (i.e., PORH) to animal models such as mice. However, blood flow measurement in small skeletal muscles of mice represents a major technical challenge.

Current technologies used for tissue blood flow measurement in mouse limb include the microsphere method [8], laser Doppler flowmetry (LDF) [9], laser Doppler imaging (LDI) [10], and arterial-spin-labeled magnetic resonance imaging (ASL-MRI) [11–13]. Although the semi-invasive microsphere method is accepted as a gold standard for the measurement of microvascular blood flow in relatively larger animals (e.g., rats), the withdrawing of arterial blood samples alters the total blood volume in smaller animals such as mice, making continuous or repeated measurements inaccurate. LDF and LDI are capable of measuring tissue blood flow, but only at the tissue surface. Very few studies have used ASL-MRI to measure blood flow in mouse skeletal muscles during PORH [11,12] because the large and costly instrumentation required for ASL-MRI precludes its frequent use. Furthermore, the reliability of ASL-MRI measurements is limited when blood flow level is low [14,15], e.g., in the resting muscles.

The emerging technology, near-infrared (NIR) diffuse correlation spectroscopy (DCS), offers a noninvasive, rapid, and low-cost alternative for the longitudinal measurement of relative change of blood flow (rBF) in deep tissues. DCS uses NIR light to directly detect the motion of red blood cells in deep microvasculature [16–18]. The relatively low tissue absorption of NIR light (650 to 950 nm) allows DCS to monitor muscle blood flow deep underneath the skin. Furthermore, DCS measurements of rBF have been extensively validated against other techniques, including LDF [19,20], Doppler ultrasound [21,22], power spectral Doppler ultrasound [23], fluorescent microsphere flow measurement [24], ASL-MRI [15], and Xenon computed tomography [25].

Although DCS has been extensively used for quantifying rBF in human skeletal muscles [15,26–31], the challenge remains to adapt it to the small size of skeletal muscles in mice. Mesquita *et al.* have recently placed a small DCS fiber-optic probe (attached to a post) on top of the mouse thigh muscle to longitudinally study muscle vascular regrowth after hindlimb ischemia induced by femoral artery ligation [32]. However, their study involved an invasive surgical procedure (i.e., femoral artery ligation), and was not intended to measure PORH responses. DCS measurements of rBF during PORH in mouse skeletal muscles have not yet been reported, which is likely due to the difficulties of probe placement and occlusive manipulation on the small mouse thigh. In this study, we developed a small fiber-optic probe and glued it on top of the mouse thigh muscle to reduce the motion artifact during occlusive manipulation. A polyvinyl chloride (PVC) tube was used on the thigh to create an arterial occlusion for 5 min. A surgical cautery pen was then used to burn (i.e., sever) the tube, allowing for rapid release of the occlusion while inducing minimal motion of the thigh. Typical PORHs were observed from the continuous DCS blood flow measurements in mouse thigh muscles.

2. Materials and Methods

A. DCS for rBF Measurement

Details about DCS theory and instrumentation can be found elsewhere [33–36]. Briefly, a four-channel DCS unit consists of a long-coherence-length (> 5 m) NIR laser diode (785 nm, 100 mW, CrystaLaser Inc., California, USA), four single-photon-counting avalanche photodiodes (APDs, Excelitas Technologies Corp., Canada), and a four-channel correlator (correlator.com, New Jersey, USA) (Fig. 1). Optical fibers connected to the laser and APD are placed on the tissue surface with a distance of millimeters to centimeters depending on the desired penetration depth of light. According to photon diffuse theory, the penetration depth of NIR light in biological tissues is approximately one half of the source-detector (S-D) separation [34,37,38]. In this study, we used an optical probe with one pair of source and detector fibers placed at an S-D separation of 6 mm, which allows for the detection of rBF deep in the thigh muscles of mice (Fig. 2). The sampling rate of DCS measurement was 0.5 Hz.

For DCS measurements, NIR light generated by the laser diode is launched into tissues through a multimode source fiber (core diameter = 200 μm). While transporting through the tissue, photons are either scattered by tissue scatterers (e.g., red blood cells, organelles, and mitochondria) or absorbed by

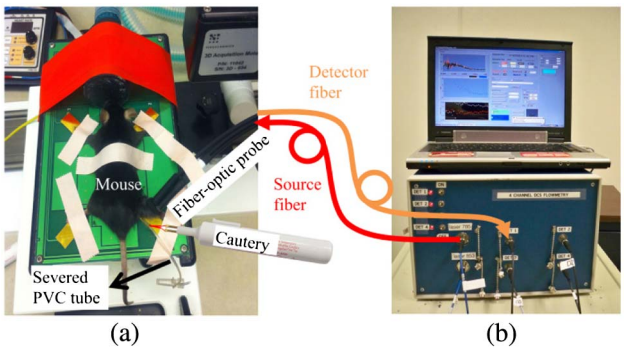

Fig. 1. (a) Animal experimental setup and (b) DCS device. The mouse was anesthetized with 1% isoflurane through inhaling and secured on a heated pad by taping the limbs. A fiber-optic probe was glued on the mouse right thigh. A surgical cautery was used to burn/cut the PVC tube. The fiber-optic probe with source and detector fibers were connected to the DCS device.

tissue absorbers (e.g., hemoglobin). Only some of the photons eventually reach the APD via a single-mode detector fiber (core diameter = 5.6 μm). The motion of moving scatterers (primarily red blood cells in microvasculature) causes light intensity fluctuation on the tissue surface, which can be detected by the APD [18,27,33]. The correlator takes the output from the APD and calculates the light intensity temporal autocorrelation function. The electric field temporal autocorrelation function derived from the measured intensity autocorrelation function satisfies the correlation diffusion equation in highly scattering media [33]. A blood flow index αD_B is extracted by fitting the electric field autocorrelation function to its analytical solution of the correlation diffusion equation. Here, D_B is the *effective* diffusion coefficient of the moving red blood cells and α (ranging from 0 to 1) is the ratio of moving scatterers to total scatterers [33,35]. The unit of DCS flow index (αD_B) is cm^2/s, which differs from the classical blood flow unit in biological tissues (ml/min/100 g). However, the percentage changes in αD_B (i.e., rBF) reported in this study have been

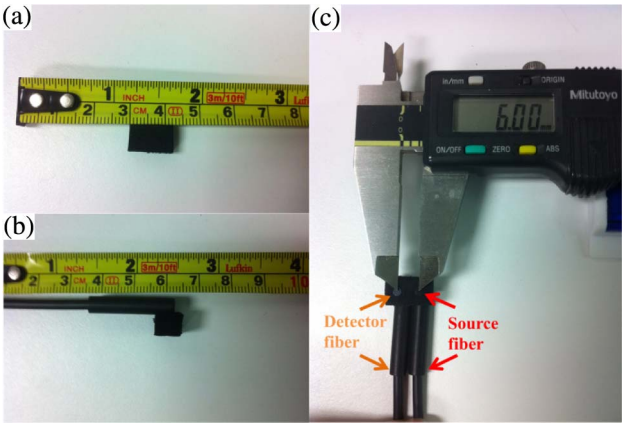

Fig. 2. Small DCS fiber-optic probe consisted of a rectangular foam pad (a), to confine the source and detector fibers (b) at a distance of 6 mm (c).

previously found to correlate well with the blood flow changes measured by many other established modalities [15,19–25], as mentioned in the Introduction section.

B. Fiber-Optic Probe Designed Particularly for Small Mouse Leg

A special fiber-optic probe was designed for use on the mouse thigh (Fig. 2). Specifically, a rectangular black foam pad was cut to match the small size of mouse thigh. Two holes were drilled in the pad to confine the source and detector fibers at a distance of 6 mm. Previous DCS measurements in human subjects often secured a big fiber-optic probe with large S-D separations (several centimeters) on the skeletal muscle using medical tape or elastic bandage [28–31]. However, medical tape is not strong enough to fix the small custom-made probe on the small thighs of the mice tested in the present study. Furthermore, an elastic bandage may result in the imposition of unwanted pressure on the soft tissues of the thigh, which may distort tissue blood flow. In this study, we first glued the foam pad on mouse right thigh, and then inserted the source and detector fibers into the pad. After the measurement, optical fibers can be easily detached from the pad for reuse and the foam pad can be removed from the mouse leg using acetone to dissolve the glue. This design allows for repeated measurements for longitudinal monitoring.

C. Animal Preparation and Experimental Protocol

The experimental protocol was approved by the Institutional Animal Care and Use Committee of University of Kentucky. Seven male low-density lipoprotein receptor deficient (LDLr-/-) mice (B6.129S7-Ldlr^{tm1Her}; Cat No. 2207) were purchased from the Jackson Laboratory (Bar Harbor, ME). Before installing the DCS probe, the mice (16 weeks old) were anesthetized with 1% isoflurane (Butler Schein), and secured in a prone position by taping the limbs on a heating pad [Fig. 1(a)]. Body temperature was kept at 37°C. The hair overlying the test site on the thigh of the right hindlimb was shaved for the installation of the fiber-optic probe.

The experimental protocol consisted of a 5 min resting baseline, a 5 min arterial occlusion, and a postocclusive period until rBF recovered to its preocclusion baseline level (Fig. 3). A real-time blood flow index (αD_B) was continuously measured by the DCS probe before, during, and after the occlusion. A loose overhand knot was wrapped around the thigh between the hip and the glued optical probe using a PVC tube (outer diameter: 0.05 in.). The occlusion was generated by manually increasing the tying force on the knot until the blood flow (monitored continuously by DCS) decreased to less than 10% of its baseline level. At the end of the 5 min occlusion, a high temperature surgical cautery pen was used to sever the PVC tubing by gently burning through it, which released the arterial occlusion rapidly without

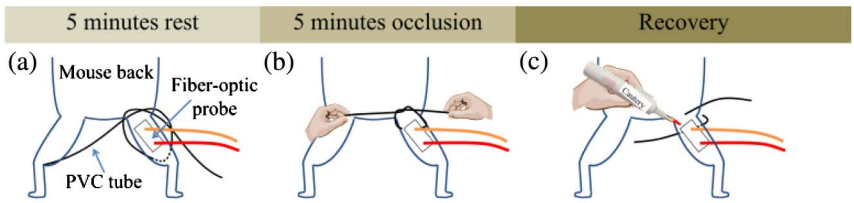

Fig. 3. Schematic showing the arterial occlusive procedure. (a) The fiber-optic probe was glued on the mouse right thigh for monitoring muscle rBF throughout the experimental procedure. The PVC tube was loosely wrapped between the hip and glued probe at rest. (b) The tying force on the tube was increased to occlude the artery for 5 min. (c) A surgical cautery was used to burn the tube and release the occlusion.

significantly interrupting the optical measurement or injuring the animal.

D. Data Analysis

Following the methods used in previous studies [15,28,30,39], rBF throughout the test procedure was calculated by normalizing the instantaneous αD_B by its baseline value, which was determined as the average value of the measurements recorded for 1 min immediately prior to the arterial occlusion. The average baseline blood flow value was assigned a value of 100%. The averaged value of rBF during 5 min occlusion, peak rBF during PORH, and time-to-peak (the time duration from the end of the occlusion to the peak rBF) were quantified for each mouse (Fig. 4). All average results over the seven mice are presented as mean ± standard deviation.

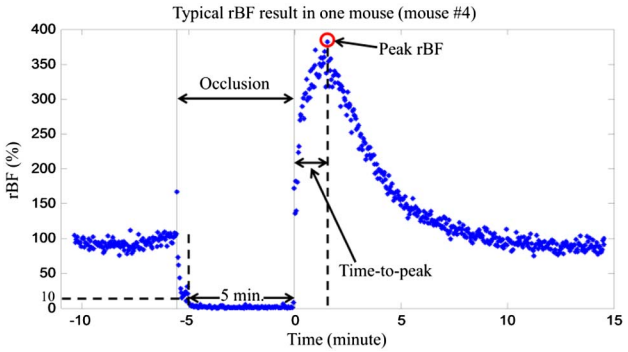

Fig. 4. Typical blood flow response during POHR in one mouse. Two vertical solid gray lines indicate the beginning and ending of the arterial occlusion, respectively. The dot inside the red circle represents the peak rBF during PORH. The time duration from the occlusion release to the peak rBF is defined as time-to-peak.

3. Results

Figure 4 shows the typical rBF response to the arterial occlusion in one mouse. Time 0 represents the time to release the occlusion. rBF decreased sharply to almost zero at the beginning of the occlusion, then maintained at a stable level (2.0 ± 1.4%) during the 5 min of occlusion. A typical PORH occurred following the release of the occlusion; rBF increased rapidly and reached its peak value (peak rBF = 381.8%) in 92 s (time-to-peak), followed by a gradual recovery period toward its baseline.

The individual rBF responses of all mice ($n = 7$) are plotted in Fig. 5. Data were aligned to Time 0 when the occlusion was released. A relatively high temporal resolution (0.5 Hz) of DCS measurements resulted in the generation of smooth rBF curves for all mice. rBF values during occlusion were consistently <10% in all mice, indicating the success of the arterial occlusion. After the release of the occlusion, all mice showed a typical PORH with relatively small intrasubject variation. Figure 6 shows the average rBF responses and variations during PORH over seven mice. Data are presented as means ± standard deviations. On average, rBF during occlusion, peak rBF, and time-to-peak were 3.1 ± 2.2%, 357.6 ± 36.3%, and 112.6 ± 35.0 s, respectively.

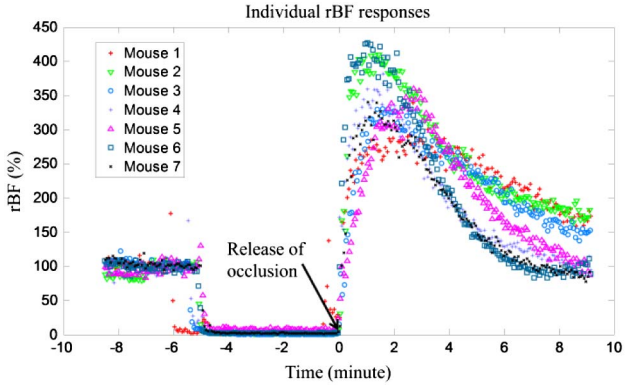

Fig. 5. Individual rBF responses during PORH. All time-course data are aligned at Time 0 when the arterial occlusion was released.

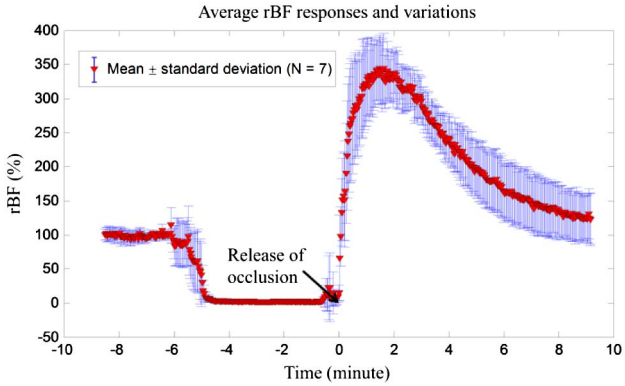

Fig. 6. Average rBF responses and variations (depicted as standard deviation bars) during PORH for $n = 7$ mice. All time-course data are aligned at Time 0 when the arterial occlusion was released.

4. Discussion and Conclusions

Quantification of skeletal muscle blood flow response during PORH has been extensively used in evaluating the vascular function of human skeletal muscle [3,7,40]. However, very few studies reported evaluating PORH in mouse skeletal muscles [11,12], which is likely due to the lack of readily available noninvasive techniques for blood flow measurements in deep muscles coupled with the challenge of measurement setup resulting from the lack of large enough test sites to conduct a PORH assessments on mice.

ASL-MRI provides noninvasive and absolute measurement of muscle blood flow in the mouse hindlimb [11–13]. However, this approach produces less reliable measurements when blood flow is low (e.g., muscle blood flow at resting baseline and during arterial occlusion) [14,15]. Without a reliable baseline measurement, the percentage change of blood flow (e.g., peak rBF) during PORH cannot be determined, which is an important parameter for the diagnosis of microvascular dysfunction due to vascular disease states (e.g., PAD) [7]. In addition, the low sampling rate of ASL-MRI measurement in mice (e.g., sampling time >10 s [11]) reduces the accuracy in the determination of response time (e.g., time-to-peak) during PORH. Furthermore, the high cost of ASL-MRI measurements limits its frequent use in research.

By contrast, DCS is a noninvasive, fast, and inexpensive tool for real-time measurement of relative blood flow changes in deep mouse muscles. The challenge of applying DCS for the study of PORH in murine muscles includes the placement of the fiber-optic probe and the application of arterial occlusion in small mouse limbs with limited space. In the present study, we adapted a small fiber-optic probe for the use on the small mouse limb (see Figs. 1 and 2). The probe pad confining the optical fibers was glued on the mouse limb to reduce the motion artifact. The detachable design separating the probe pad and optical fibers allows for the reuse of optical fibers. The foam pad can be removed from the mouse leg using acetone to dissolve the glue, which allows for repeated (i.e., longitudinal) measurements.

Another challenge is to perform the arterial occlusion with minimum disturbance to blood flow measurements. Although commercial inflatable tail cuffs have been frequently used in mouse models [41], a cuff for use on the mouse thigh is not available. Bertoldi *et al.* used two threads wrapped around the mouse thigh and pulled tightly closed by two weights to induce arterial occlusion on the mouse thigh inside an ASL-MRI coil; the occlusion was released by removing the weights [11]. However, it is difficult to determine how much weight for each individual mouse should be applied to occlude the artery completely without causing damage to the tissues underneath the threads. Furthermore, the success of the occlusion cannot be judged from an online (i.e., real time) measure or during postprocessing of blood flow data since ASL-MRI measurements are not reliable when tissue blood flow is low during occlusion [14,15]. In the present study, we occluded the arterial blood flow by tying a flexible PVC tube around the mouse thigh (see Fig. 3). The tying force was gently increased and continuously monitored by the DCS device. Once the blood flow reached a level of less than 10% of its baseline value (i.e., rBF <10%), the tying force was kept constant for 5 min. The occlusion was then rapidly released by cutting the PVC tube using a surgical cautery pen.

Overall, the new methods used in the present study minimized motion artifact (by gluing the probe on the mouse thigh), ensured the success of the occlusion (by monitoring the blood flow level), and obtained consistent flow responses during PORH (by rapidly releasing the occlusion force).

The results obtained from the present study were compared to the limited available blood flow data in mouse thigh during PORH measured by ASL-MRI [11]. Results from two other studies in mouse skeletal muscle using ASL-MRI are excluded from the comparison as one did not report quantitative responses during PORH [12] and the other monitored blood flow during electrical stimulation [13]. Similar dynamic trends/patterns throughout the arterial occlusion procedure were observed in both the measurements of the present study (see Figs. 4 and 5) in comparison with those reported in the literature (see Fig. 6 in Bertoldi *et al.* [11]).

To facilitate a quantitative comparison between the measurements of the present study and those of Bertoldi *et al.* [11], the reported absolute blood flow values measured for PORH by ASL-MRI were normalized to their baseline values before the occlusion, even though these baseline values might not be reliable due to the low level of blood flow. Table 1 lists the comparison results. The peak values of rBF in mouse thigh muscles quantified by DCS ($357.6 \pm 36.3\%$) and ASL-MRI ($387.5 \pm 150.0\%$) were similar, but the data variation of ASL-MRI measurements ($\pm 150.0\%$) was much greater than that of DCS measurements ($\pm 36.3\%$). Although it is unclear why the average time-to-peak measured by DCS (112.6 ± 35.0 s) was ~2.3 times longer than that measured by ASL-MRI (48 ± 27 s), the differences between the two studies may have contributed to the discrepancy observed. These differences (see Table 1) include the strain and age of mice, tissue heterogeneity, occlusion duration and data sampling time, reliability of baseline/occlusion measurements, and success of arterial occlusion. In addition, the contact DCS measurements (in contrast to the noncontact ASL-MRI measurements) may have altered skeletal muscle blood flow responses by a potential light pressure imposed by the fiber-optic probe on the soft muscle tissues [15].

In conclusion, we have successfully adapted our novel DCS system for noninvasive evaluation of blood flow responses during PORH in mouse thigh muscles. We also showed that the thigh is a feasible location to conduct DCS assessment of muscle blood flow regulation, e.g., during PORH. DCS-based rBF

Table 1. Comparison of Blood Flow Responses During PORH Measured by DCS and ASL-MRI

	DCS (cm^2/s) Cheng *et al.*, 2013 (the present study)	ASL-MRI (ml/ min /100 g) Bertoldi *et al.*, 2008 [11]
Number of mice	$N = 7$	$N = 6$
Strain of mice	LDLr-/-(background: C57BL/6J)	Cross-breed of MNRI and C57BL/6J
Age of mice	16 weeks	20 weeks
Data sampling time	2 s	>10 s
Occlusion duration	5 min	3 min
Baseline blood flow/rBF	$100.0 \pm 0.0\%$	16.0 ± 11.1 (assigned to be $100.0 \pm 69.4\%$)
Occlusion blood flow/rBF	$3.1 \pm 2.2\%$	-1.7 ± 7.7 (equivalent to $-10.6 \pm 48.1\%$)
Peak blood flow/rBF	$357.6 \pm 36.3\%$	62 ± 24 (equivalent to $387.5 \pm 150.0\%$)
Time-to-peak	112.6 ± 35.0 s	48 ± 27 s

measurements in the mouse thigh showed a typical PORH response pattern that is consistent with the absolute blood flow measurements by ASL-MRI in the literature. Peak values of rBF during PORH measured by DCS and ASL-MRI were similar whereas the values for time-to-peak were quite different. Simultaneous measurements by the two techniques, as we did previously in human skeletal muscles [15], are needed to identify the factors that may have caused this discrepancy. In the future, we intend to test the ability of DCS to detect changes in microcirculatory function for mouse models of vascular diseases (e.g., hypercholesterolemia, diabetes, PAD) and explore the diagnostic and research value of DCS for quantifying deep muscle blood flow regulation.

This work was supported by an American Heart Association (Nos. 09BGIA2250309 and 09BGIA2350015) and a National Science Foundation Kentucky EPSCoR-Bioengineering Initiative grant (No. 0814194). We thank the Saha Cardiovascular Research Center at the University of Kentucky for the use of their animal research facility.

†These authors contributed equally to this work.

References

1. Z. Guo, W. Su, H. Pang, and M. Gong, "COX-2 up-regulation and vascular smooth muscle contractile hyperreactivity in spontaneous diabetic db/db mice," Diabetes **54**, 190 (2004).
2. A. J. Rufaihah, N. F. Huang, S. Jame, J. C. Lee, H. N. Nguyen, B. Byers, A. De, J. Okogbaa, M. Rollins, R. Reijo-Pera, S. S. Gambhir, and J. P. Cooke, "Endothelial cells derived from human iPSCS increase capillary density and improve perfusion in a mouse model of peripheral arterial disease," Arterioscler. Thromb. Vasc. Biol. **31**, E72–E79 (2011).
3. A. L. Huang, A. E. Silver, E. Shvenke, D. W. Schopfer, E. Jahangir, M. A. Titas, A. Shpilman, J. O. Menzoian, M. T. Watkins, J. D. Raffetto, G. Gibbons, J. Woodson, P. M. Shaw, M. Dhadly, R. T. Eberhardt, J. F. Keaney, N. Gokce, and J. A. Vita, "Predictive value of reactive hyperemia for cardiovascular events in patients with peripheral arterial disease undergoing vascular surgery," Arterioscler. Thromb. Vasc. Biol. **27**, 2113–2119 (2007).
4. A. E. Caballero, S. Arora, R. Saouaf, S. C. Lim, P. Smakowski, J. Y. Park, G. L. King, F. W. LoGerfo, E. S. Horton, and A. Veves, "Microvascular and macrovascular reactivity is reduced in subjects at risk for type 2 diabetes," Diabetes **48**, 1856–1862 (1999).
5. J. H. Lombard and B. R. Duling, "Multiple mechanisms of reactive hyperemia in arterioles of the hamster-cheek pouch," Am. J. Physiol. **241**, H748–H755 (1981).
6. M. Roustit and J. L. Cracowski, "Non-invasive assessment of skin microvascular function in humans: an insight into methods," Microcirculation **19**, 47–64 (2012).
7. M. H. Criqui, A. Fronek, E. Barrettconnor, M. R. Klauber, S. Gabriel, and D. Goodman, "The prevalence of peripheral arterial-disease in a defined population," Circulation **71**, 510–515 (1985).
8. F. W. Prinzen and J. B. Bassingthwaighte, "Blood flow distributions by microsphere deposition methods," Cardiovasc. Res. **45**, 13–21 (2000).
9. C. Emanueli, A. Minasi, A. Zacheo, J. Chao, L. Chao, M. B. Salis, S. Straino, M. G. Tozzi, R. Smith, L. Gaspa, G. Bianchini, F. Stillo, M. C. Capogrossi, and P. Madeddu, "Local delivery of human tissue kallikrein gene accelerates spontaneous angiogenesis in mouse model of hindlimb ischemia," Circulation **103**, 125–132 (2001).
10. A. Helisch, S. Wagner, N. Khan, M. Drinane, S. Wolfram, M. Heil, T. Ziegelhoeffer, U. Brandt, J. D. Pearlman, H. M. Swartz, and W. Schaper, "Impact of mouse strain differences in innate hindlimb collateral vasculature," Arterioscler. Thromb. Vasc. Biol. **26**, 520–526 (2005).
11. D. Bertoldi, P. Loureiro de Sousa, Y. Fromes, C. Wary, and P. G. Carlier, "Quantitative, dynamic and noninvasive determination of skeletal muscle perfusion in mouse leg by NMR arterial spin-labeled imaging," Magn. Reson. Imaging **26**, 1259–1265 (2008).
12. P. G. Carlier, D. Bertoldi, C. Baligand, C. Wary, and Y. Fromes, "Muscle blood flow and oxygenation measured by NMR imaging and spectroscopy," NMR Biomed. **19**, 954–967 (2006).
13. C. Baligand, C. Wary, J. C. Menard, E. Giacomini, J. Y. Hogrel, and P. G. Carlier, "Measuring perfusion and bioenergetics simultaneously in mouse skeletal muscle: a multiparametric functional-NMR approach," NMR Biomed. **24**, 281–290 (2011).
14. E. T. Petersen, I. Zimine, Y. C. L. Ho, and X. Golay, "Non-invasive measurement of perfusion: a critical review of arterial spin labelling techniques," Br. J. Radiol. **79**, 688–701 (2006).
15. G. Yu, T. Floyd, T. Durduran, C. Zhou, J. J. Wang, J. A. Detre, and A. G. Yodh, "Validation of diffuse correlation spectroscopy for muscle blood flow with concurrent arterial spin labeled perfusion MRI," Opt. Express **15**, 1064–1075 (2007).
16. D. J. Pine, D. A. Weitz, P. M. Chaikin, and E. Herbolzheimer, "Diffusing-wave spectroscopy," Phys. Rev. Lett. **60**, 1134–1137 (1988).
17. G. Maret and P. E. Wolf, "Multiple light scattering from disordered media. The effect of Brownian motion of scatterers," Z. Phys. B **65**, 409–413 (1987).
18. D. A. Boas, L. E. Campbell, and A. G. Yodh, "Scattering and imaging with diffusing temporal field correlations," Phys. Rev. Lett. **75**, 1855–1858 (1995).
19. T. Durduran, *Non-Invasive Measurements of Tissue Hemodynamics with Hybrid Diffuse Optical Methods* (University of Pennsylvania, 2004).
20. Y. Shang, L. Chen, M. Toborek, and G. Yu, "Diffuse optical monitoring of repeated cerebral ischemia in mice," Opt. Express **19**, 20301–20315 (2011).
21. E. M. Buckley, N. M. Cook, T. Durduran, M. N. Kim, C. Zhou, R. Choe, G. Yu, S. Shultz, C. M. Sehgal, D. J. Licht, P. H. Arger,

M. E. Putt, H. Hurt, and A. G. Yodh, "Cerebral hemodynamics in preterm infants during positional intervention measured with diffuse correlation spectroscopy and transcranial Doppler ultrasound," Opt. Express **17**, 12571–12581 (2009).
22. N. Roche-Labarbe, S. A. Carp, A. Surova, M. Patel, D. A. Boas, P. E. Grant, and M. A. Franceschini, "Noninvasive optical measures of CBV, StO(2), CBF index, and rCMRO(2) in human premature neonates' brains in the first six weeks of life," Hum. Brain Mapp. **31**, 341–352 (2010).
23. G. Yu, T. Durduran, C. Zhou, H. W. Wang, M. E. Putt, H. M. Saunders, C. M. Sehgal, E. Glatstein, A. G. Yodh, and T. M. Busch, "Noninvasive monitoring of murine tumor blood flow during and after photodynamic therapy provides early assessment of therapeutic efficacy," Clin. Cancer Res. **11**, 3543–3552 (2005).
24. C. Zhou, S. Eucker, T. Durduran, G. Yu, J. Ralston, S. Friess, R. Ichor, S. Margulies, and A. G. Yodh, "Diffuse optical monitoring of hemodynamic changes in piglet brain with closed head injury," J. Biomed. Opt. **14**, 034015 (2009).
25. M. N. Kim, T. Durduran, S. Frangos, B. L. Edlow, E. M. Buckley, H. E. Moss, C. Zhou, G. Yu, R. Choe, E. Maloney-Wilensky, R. L. Wolf, M. S. Grady, J. H. Greenberg, J. M. Levine, A. G. Yodh, J. A. Detre, and W. A. Kofke, "Noninvasive measurement of cerebral blood flow and blood oxygenation using near-infrared and diffuse correlation spectroscopies in critically brain-injured adults," Neurocrit. Care **12**, 173–180 (2010).
26. Y. Shang, T. B. Symons, T. Durduran, A. G. Yodh, and G. Yu, "Effects of muscle fiber motion on diffuse correlation spectroscopy blood flow measurements during exercise," Biomed. Opt. Express **1**, 500–511 (2010).
27. G. Yu, T. Durduran, G. Lech, C. Zhou, B. Chance, E. R. Mohler III, and A. G. Yodh, "Time-dependent blood flow and oxygenation in human skeletal muscles measured with noninvasive near-infrared diffuse optical spectroscopies," J. Biomed. Opt. **10**, 024027 (2005).
28. Y. Shang, Y. Zhao, R. Cheng, L. Dong, D. Irwin, and G. Yu, "Portable optical tissue flow oximeter based on diffuse correlation spectroscopy," Opt. Lett. **34**, 3556–3558 (2009).
29. G. Yu, Y. Shang, Y. Zhao, R. Cheng, L. Dong, and S. P. Saha, "Intraoperative evaluation of revascularization effect on ischemic muscle hemodynamics using near-infrared diffuse optical spectroscopies," J. Biomed. Opt. **16**, 027004 (2011).
30. K. Gurley, Y. Shang, and G. Yu, "Noninvasive optical quantification of absolute blood flow, blood oxygenation, and oxygen consumption rate in exercising skeletal muscle," J. Biomed. Opt. **17**, 075010 (2012).
31. N. Munk, B. Symons, Y. Shang, R. Cheng, and G. Yu, "Noninvasively measuring the hemodynamic effects of massage on skeletal muscle: a novel hybrid near-infrared diffuse optical instrument," J. Bodywave Mov. Ther. **16**, 22–28 (2012).
32. R. C. Mesquita, N. Skuli, M. N. Kim, J. M. Liang, S. Schenkel, A. J. Majmundar, M. C. Simon, and A. G. Yodh, "Hemodynamic and metabolic diffuse optical monitoring in a mouse model of hindlimb ischemia," Biomed. Opt. Express **1**, 1173–1187 (2010).
33. D. A. Boas and A. G. Yodh, "Spatially varying dynamical properties of turbid media probed with diffusing temporal light correlation," J. Opt. Soc. Am. A **14**, 192–215 (1997).
34. D. Irwin, L. Dong, Y. Shang, R. Cheng, M. Kudrimoti, S. D. Stevens, and G. Yu, "Influences of tissue absorption and scattering on diffuse correlation spectroscopy blood flow measurements," Biomed. Opt. Express **2**, 1969–1985 (2011).
35. C. Cheung, J. P. Culver, K. Takahashi, J. H. Greenberg, and A. G. Yodh, "In vivo cerebrovascular measurement combining diffuse near-infrared absorption and correlation spectroscopies," Phys. Med. Biol. **46**, 2053–2065 (2001).
36. J. Li, M. Ninck, L. Koban, T. Elbert, J. Kissler, and T. Gisler, "Transient functional blood flow change in the human brain measured noninvasively by diffusing-wave spectroscopy," Opt. Lett. **33**, 2233–2235 (2008).
37. S. Fantini, M. A. Franceschini, and E. Gratton, "Semi-infinite-geometry boundary-problem for light migration in highly scattering media–a frequency-domain study in the diffusion-approximation," J. Opt. Soc. Am. B **11**, 2128–2138 (1994).
38. R. Cheng, Y. Shang, D. Hayes, S. P. Saha, and G. Yu, "Noninvasive optical evaluation of spontaneous low frequency oscillations in cerebral hemodynamics," NeuroImage **62**, 1445–1454 (2012).
39. Y. Shang, K. Gurley, B. Symons, D. Long, R. Srikuea, L. J. Crofford, C. A. Peterson, and G. Yu, "Noninvasive optical characterization of muscle blood flow, oxygenation, and metabolism in women with fibromyalgia," Arthritis Res. Ther. **14**, R236 (2012).
40. A. Fronek, K. Johansen, R. B. Dilley, and E. F. Bernstein, "Ultrasonographically monitored postocclusive reactive hyperemia in the diagnosis of peripheral arterial occlusive disease," Circulation **48**, 149–152 (1973).
41. J. H. Krege, J. B. Hodgin, J. R. Hagaman, and O. Smithies, "A noninvasive computerized tail-cuff system for measuring blood pressure in mice," Hypertension **25**, 1111–1115 (1995).